

# We are IntechOpen, the world's leading publisher of Open Access books Built by scientists, for scientists

5,000

Open access books available

124,000

International authors and editors

140M

Downloads

Our authors are among the

154

Countries delivered to

TOP 1%

most cited scientists

12.2%

Contributors from top 500 universities



WEB OF SCIENCE™

Selection of our books indexed in the Book Citation Index  
in Web of Science™ Core Collection (BKCI)

Interested in publishing with us?  
Contact [book.department@intechopen.com](mailto:book.department@intechopen.com)

Numbers displayed above are based on latest data collected.  
For more information visit [www.intechopen.com](http://www.intechopen.com)



---

# Energy Efficient Indirect Evaporative Air Cooling

---

Xin Cui, Xiaohu Yang, Yanjun Sun,  
Xiangzhao Meng and Liwen Jin

Additional information is available at the end of the chapter

<http://dx.doi.org/10.5772/intechopen.79223>

---

## Abstract

An energy-saving and environmentally friendly air-conditioning method has been proposed. The key component is a novel indirect evaporative heat exchanger (IEHX) based on the M-cycle. In this design, the compact IEHX is able to produce sub-wet-bulb cooling and reduce the air temperature approaching dew-point temperature. This chapter aims to achieve a fundamental understanding of the novel IEHX. A numerical model has been developed and validated by comparing the simulated outlet air conditions against experimental data. The model showed a good agreement with the experimental findings. Employing the validated numerical model, we have theoretically investigated the heat and mass transfer behavior occurred in the IEHX. The detailed cooling process has been analyzed on the psychrometric chart. In addition, the effects of varying inlet conditions and airflow passage dimensions on the cooling efficiency have been studied. By analyzing the thermal performance of the IEHX, we have provided possible suggestions to improve the performance of the dew-point cooler and enable it to attain higher cooling effectiveness.

**Keywords:** air conditioning, indirect evaporative cooling, heat exchanger, numerical simulation, heat and mass transfer

---

## 1. Introduction

The evaporative cooling technique takes the advantage of water evaporation to achieve cooling effect. As a potential alternative to the conventional mechanical vapor compression system, it has drawn great attention for building cooling applications.

An indirect evaporative cooling system is able to produce the cool air without moist change. For a typical indirect evaporative heat exchanger (IEHX), the primary air (or product air) and

the secondary air (or working air) flow in separate passages. The secondary air in wet channel acts as a heat sink by absorbing heat due to water evaporation.

The evaporative cooling system has the following advantages over the current mechanical vapor compression system [1–4]: (1) energy and cost savings; (2) reducing peak power requirements; (3) no CFCs; (4) reducing pollutant releases; and (5) easily incorporation with existing systems. On the other hand, the traditional IEHX shows the following limitations: (1) the air humidity increases in direct evaporative cooling systems resulting in uncomfortable indoor thermal environment for humans; (2) the indirect evaporative cooling system generally has a low cooling efficiency [5]; and (3) the theoretical ultimate cooled air temperature is the wet-bulb temperature.

To further enhance the cooling performance of conventional IEHX, research works have proposed a novel regenerative IEHX, which can cool the air below its wet-bulb temperature [1]. Since this design was proposed by Maisotsenko, the airflow arrangement is also named as M-cycle [2, 6]. Several studies have theoretically and experimentally investigated the dew-point evaporative cooling system [7–9]. This type of IEHX is able to branch part of the pre-cooled primary air into the wet channel [10, 11].

In order to investigate the cooling performance of a regenerative IEHX, analytical models have been developed based on modified effectiveness-NTU method [10, 12]. In addition, numerical simulations have been carried out to study the impact of key parameters on a counter-flow IEHX [13–15]. Anisimov and Pandelidis [16] presented a numerical study analyzing the indirect evaporative cooler with four different configurations. Zhao et al. [17] conducted a numerical study on a novel dew-point IEHX. According to the simulation results, the wet-bulb effectiveness of the IEHX was greatly influenced by the dimension of the airflow passages, the inlet air velocity, and working-to-intake-air ratio. The cooler achieved the highest wet-bulb effectiveness of 1.3 for a typical summer condition in the UK. Moshari and Heidarinejad [18] developed a numerical model and solved the governing equations by using finite difference method in MATLAB. The regenerative evaporative heat exchanger has been demonstrated to provide sub-wet-bulb cooling. Jradi and Riffat [19] conducted an experimental and numerical investigation on a dew-point evaporative cooling system. An optimized design of the indirect evaporative heat exchanger has been presented to obtain a dew-point effectiveness of 78%. Ham and Jeong [20] proposed a novel design on dew-point evaporative heat exchanger to address the issues of complex ventilation control and energy waste. Moshari et al. [21] investigated indirect evaporative cooling systems with one- and two-stage to analyze the optimum configuration by considering the cooling effectiveness, water consumption and thermal comfort. Chen et al. [22] developed an analytical model to study the heat and mass transfer process in an indirect evaporative cooler as a pre-cooling device in tropical areas. The model was established taking account of the condensation in the dry channels. Woods and Kozubal [23] conducted an experimental and numerical study on a desiccant-enhanced air conditioner by combining a dew-point evaporative heat exchanger and a desiccant dehumidifier. The second stage of this air conditioner was a counter-flow regenerative IEHX, which had a similar configuration compared with the IEHX designed by Zhao et al. [17] and Riangvilaikul and Kumar [24].

In this chapter, we first introduce the design of novel indirect evaporative heat exchangers, followed by the mathematical description, which was employed to study the air treatment process in the IEHX. An experimental study was then conducted to validate the computational model. Finally, the validated model was used to study the cooling performance of the novel dew-point IEHX and to investigate the impact of several influential parameters.

## 2. Description of novel indirect evaporative heat exchanger

In this section, we introduce two types of IEHX. The first type is a counter-flow regenerative IEHX. The other one is a novel dew-point IEHX based on the modification of the M-cycle arrangement.

The schematic of a one-unit channel pair of a typical counter-flow regenerative IEHX is shown in **Figure 1**. A number of this type of channel pairs is stacked to form the structure of the IEHX. The intake air flows in alternative primary channels (dry channels). Before the outlet of the dry channel, a part of the primary air is diverted into the secondary channel (wet channel). The primary air in the IEHX can be cooled along the flow passages without changing the humidity ratio.

**Figure 2** illustrates the airflow in novel dew-point IEHX in terms of a one-unit channel pair. It comprises a product channel and adjacent working channels. By spraying water in working wet channels, inner surfaces are maintained in wet conditions. The working channel employs a closed-loop arrangement. The working air firstly enters the working dry channels, and it is then recirculated into the wet channels. The configuration is able to pre-cool the working air before entering the wet side. Therefore, at the recirculation point of the working channel, the air stream achieves a high cooling capacity as a result of a lower wet-bulb temperature compared with the inlet air. Theoretically, the outlet temperature of product air can be reduced toward its dew-point temperature.

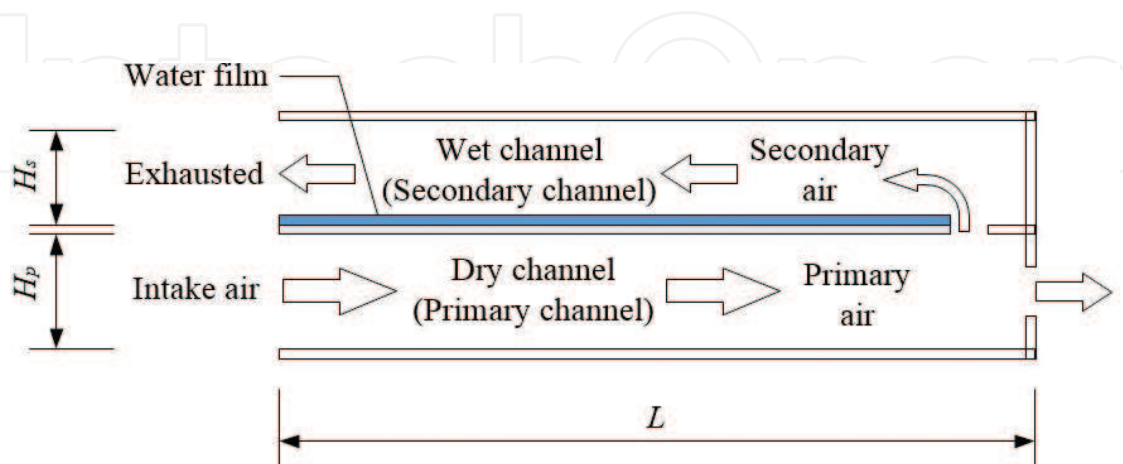


**Figure 1.** Schematic of a one-unit channel pair of a typical counter-flow regenerative indirect evaporative heat exchanger.

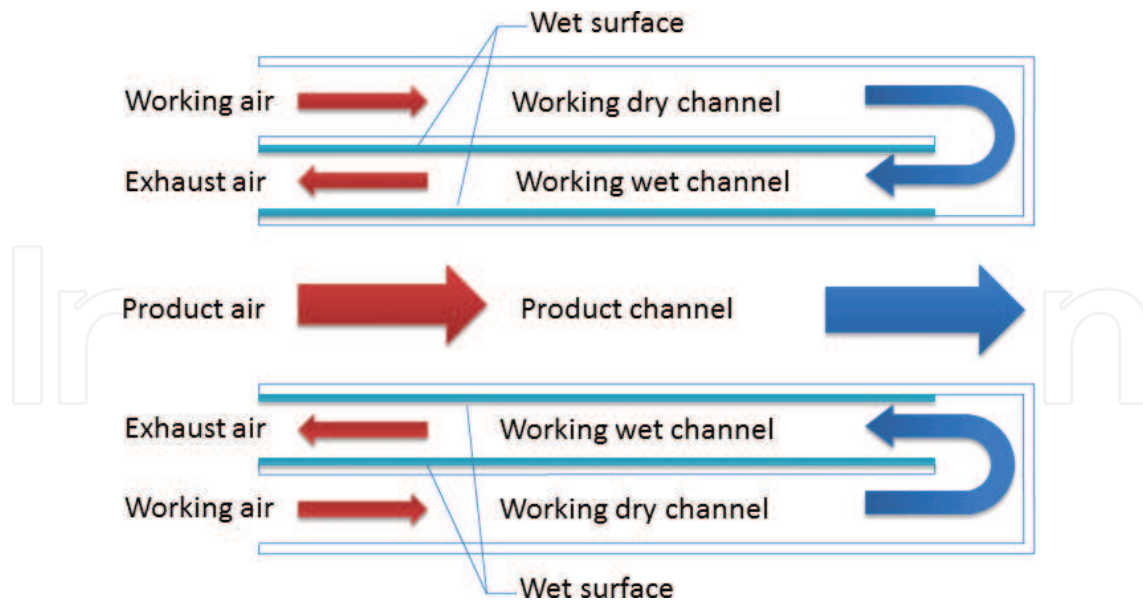


**Figure 2.** Schematic of the novel dew-point IEHX (one-unit channel pair).

### 3. Mathematical modeling

To develop a mathematical model predicting the air treatment performance in the IEHX, the following assumptions are considered: (1) the airflow is steady and incompressible; (2) the channel height is comparatively small; (3) the airflow is fully developed and laminar; (4) the surface of wet channel is covered with a thin water film; and (5) the outer surface is insulated.

The moist air flowing in both the working channel and the product channel is governed by the following equations [9].

The continuity equation:

$$\frac{\partial u_a}{\partial x} + \frac{\partial v_a}{\partial y} = 0 \tag{1}$$

Momentum conservation equation:

$$u_a \frac{\partial u_a}{\partial x} + v_a \frac{\partial u_a}{\partial y} = -\frac{1}{\rho_a} \frac{dp}{dx} + \nu_a \frac{\partial^2 u_a}{\partial y^2} \tag{2}$$

Energy conservation equation:

$$u_a \frac{\partial T_a}{\partial x} + v_a \frac{\partial T_a}{\partial y} = \alpha_a \frac{\partial^2 T_a}{\partial y^2} \tag{3}$$

Equation of species diffusion for water vapor is expressed as

$$u_a \frac{\partial c_a}{\partial x} + v_a \frac{\partial c_a}{\partial y} = D_a \frac{\partial^2 c_a}{\partial y^2} \quad (4)$$

The inlet boundary conditions of the air are indicated as

$$u_a = u_{a,in}, \quad v_a = 0, \quad T_a = T_{a,in}, \quad c_a = c_{a,in} \quad (5)$$

At the air-water interface, the moist air is assumed to be saturated with the water film temperature. The vapor pressure of the saturated moist air can be expressed as a function of temperature using the following equation [25]:

$$\ln P_{sat} = \frac{C_1}{T_w} + C_2 + C_3 T_w + C_4 T_w^2 + C_5 T_w^3 + C_6 \ln T_w \quad (6)$$

where  $C_1 = -5.800220 \times 10^3$ ,  $C_2 = 1.391499 \times 10^3$ ,  $C_3 = -4.864023 \times 10^{-2}$ ,  $C_4 = 4.176476 \times 10^{-5}$ ,  $C_5 = -1.445209 \times 10^{-8}$ ,  $C_6 = 6.545967 \times 10^3$ , and  $T_w$  is the absolute temperature of water film.

The water vapor concentration is specified as

$$c_a = \frac{P_{sat}(T_w)}{RT_w} \quad (7)$$

where  $P_{sat}(T_w)$  is the saturated vapor pressure at the absolute temperature of the water film. The evaporation rate of water is determined by the gradient diffusion as:

$$m_v = M_{H_2O} D_a \left( \frac{\partial c_a}{\partial y} \right)_w \quad (8)$$

As a result, the interfacial condition at the water film surface in the working wet channel is given as

$$u_a = 0, \quad v_a = 0 \quad (9)$$

$$-k_w \frac{dT_w}{dy} = -k_a \frac{dT_a}{dy} + M_{H_2O} h_{fg} D_a \frac{\partial c_a}{\partial y} \quad (10)$$

To evaluate the cooling efficiency of the indirect evaporative heat exchangers, following expressions (wet-bulb effectiveness and dew-point effectiveness) are defined.

$$\varepsilon_{wb} = \frac{T_{a,in} - T_{a,out}}{T_{a,in} - T_{wb,in}} \quad (11)$$

$$\varepsilon_{dew} = \frac{T_{a,in} - T_{a,out}}{T_{a,in} - T_{dew,in}} \quad (12)$$



4. Experimental study

A prototype of the plate-type counter-flow regenerative IEHX was fabricated as schematically illustrated in **Figure 3**. The one-unit channel pair comprises a product channel and two adjacent working channels. The intake air, which consists of both the working air and the product air, flows into the product channel (dry channel). At the end of the product channel, part of the product air is branched into the adjacent working wet channels by passing through the perforated plates. The dimensions for the counter-flow regenerative IEHX are listed in **Table 1**.

The schematic of the experimental setup for the IEHX is shown in **Figure 4**. A variable speed blower, which was used to control the intake airflow rate, was equipped at the inlet of the IEHX. The intake air temperature was adjusted by a heater before the blower. The measured parameters included the air temperature, humidity, and velocity.

Thermistors with accuracies of  $\pm 0.1^{\circ}\text{C}$  were employed to measure the air dry-bulb temperature. The probes were inserted into the center of the airflow passages to measure the relative

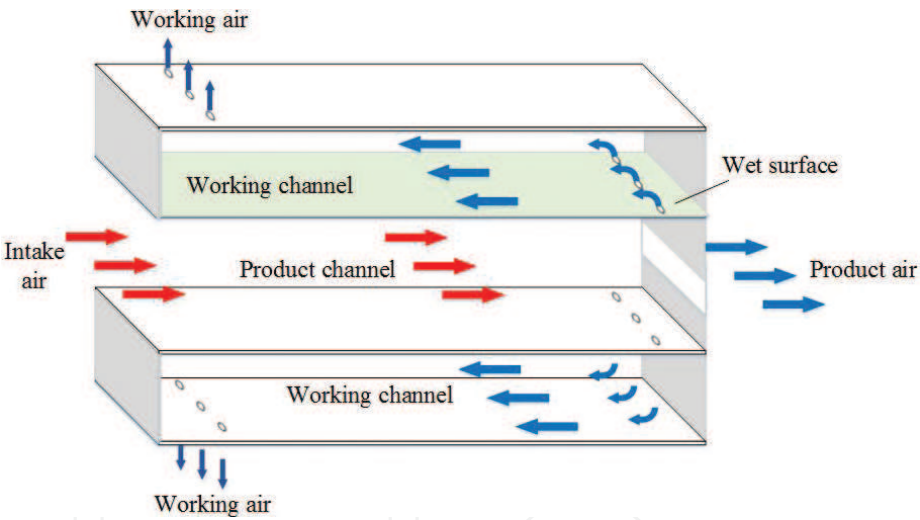


**Figure 3.** Schematic of the counter-flow regenerative IEHX.

Dimension	Symbol	Value	Units
Product channel gap	$H_{product}$	10	mm
Working channel gap	$H_{working}$	6	mm
Channel length	$L$	750	mm
Channel width	$W$	300	mm
Wall thickness	$\delta_p$	0.3	mm
Wick thickness	$\delta_{wi}$	0.2	mm

**Table 1.** Specifications for the counter-flow regenerative IEHX.

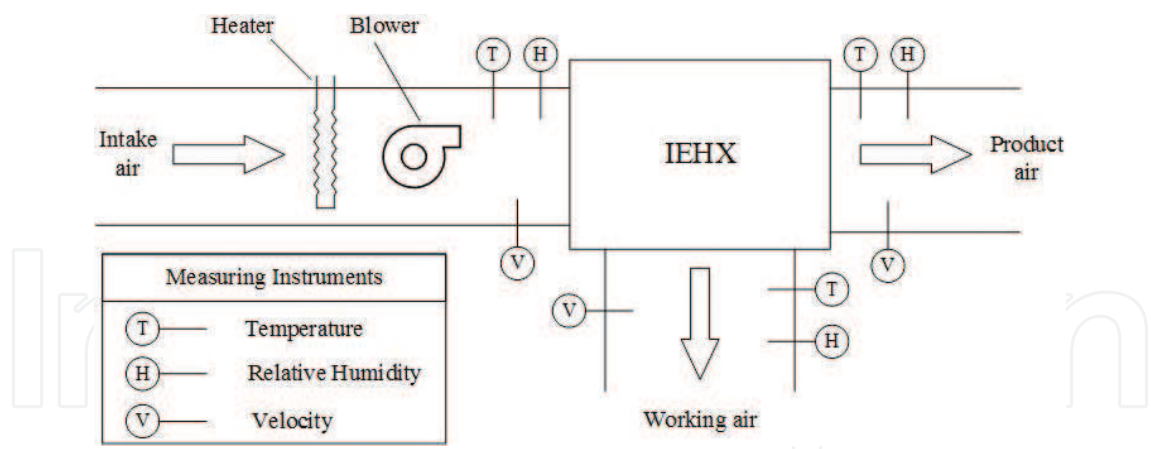


Figure 4. Schematic diagram of the experimental setup.

	Flow rate I	Flow rate II
Flow rate of intake air (L/s)	4.5	6
Velocity of product air (m/s)	1.5	2.0
Velocity of working air (m/s)	1.0	1.3
Inlet air humidity ratio (g/kg)	10	10
Inlet air temperature (°C)	22–29	22–29

Table 2. Operating condition of the counter-flow regenerative IEHX.

humidity and velocity of the air stream. The measured data were recorded using a data acquisition unit.

The experimental study was carried out to study the performance of the IEHX under varying inlet conditions. The inlet air velocity and temperature were adjusted to a stable condition by controlling the air blower and the heater. The operating conditions in this study were presented in Table 2.

## 5. Results and discussion

### 5.1. Model validation

The experimental data were first employed to validate the numerical model for the regenerative IEHX. The experimental condition was replicated in the simulation. Figure 5 illustrates the comparison between the calculated outlet air temperature and the experimental results. The numerical model shows a good agreement within a maximum discrepancy about 5%.

The numerical model was further validated against experimental data presented by Woods and Kozubal [23, 26]. The experimental study was conducted for an M-cycle indirect evaporative heat exchanger. The supply air temperatures were measured under different operating



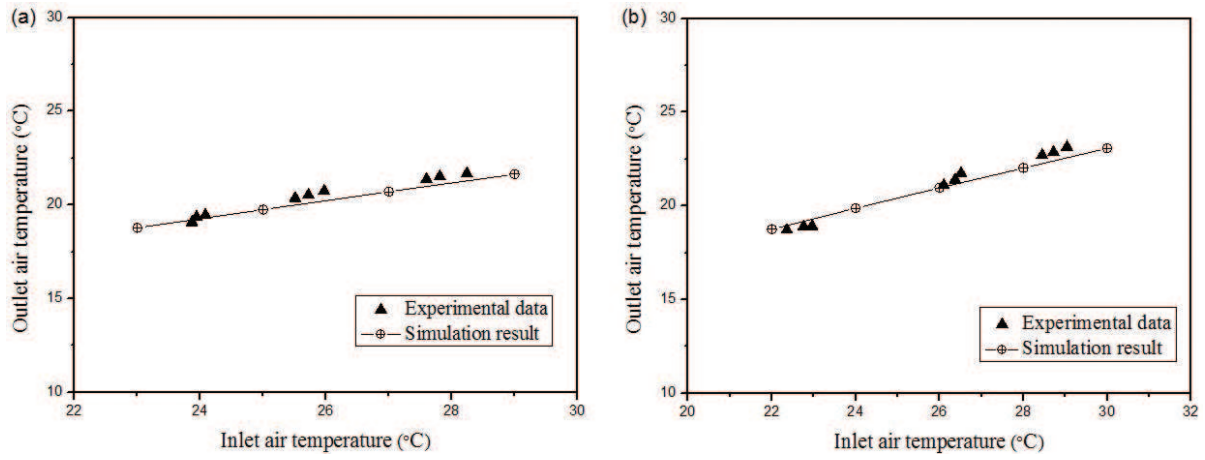


**Figure 5.** Validation 1: comparison between modeled results and experimental data on the counter-flow regenerative IEHX (a) flow rate of intake air is 4.5 L/s; (b) flow rate of intake air is 6 L/s.

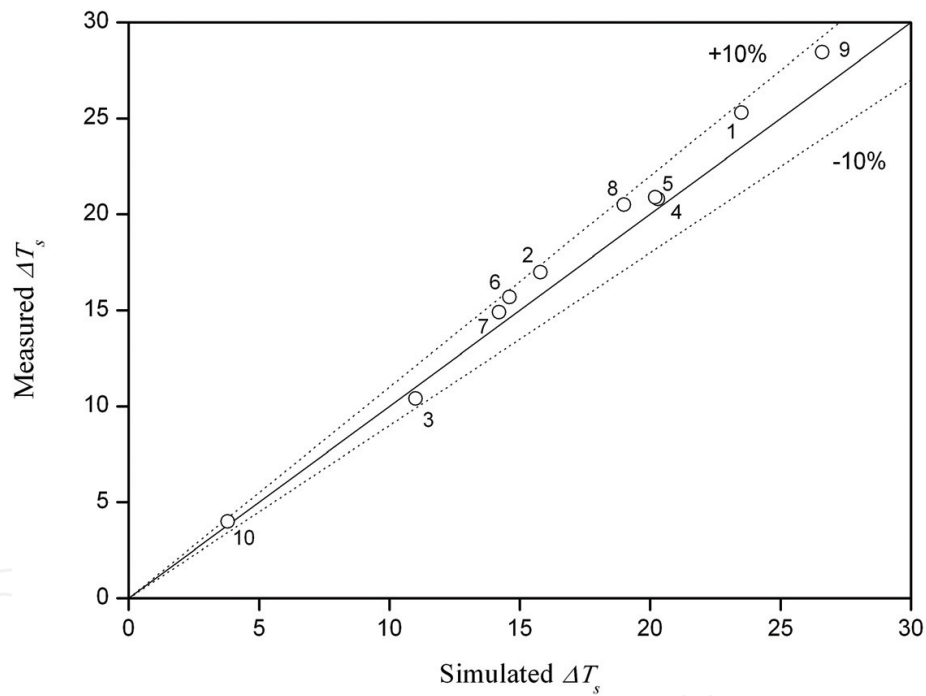


**Figure 6.** Validation 2: compare the supply air temperature change.

conditions. The validation was performed by comparing the simulated supply air temperature reduction with the experimental data. The discrepancy was within  $\pm 10\%$  as shown in **Figure 6**.

By comparing the simulated results with experimental data, we can draw the conclusion that the validation has demonstrated the capability of the numerical model to theoretically investigate the cooling process for the IEHX.

5.2. Psychrometric analysis of the cooling process

By using the validated model, we investigated the air treatment process of the novel dew-point IEHX. Simulations were carried out to predict the states of air stream in the flow passages of the cooler [5]. The assumed inlet conditions were as follows: the dry-bulb temperature was 35°C and the humidity ratio was 10 g/kg for both working air and product air. The geometry parameter and the air velocity were maintained as the pre-set conditions as shown in **Table 3**.

The psychrometric analysis of the air conditions in the novel dew-point IEHX is shown in **Figure 7**. The inlet conditions for both the working air (point W1 in **Figure 7**) and the product

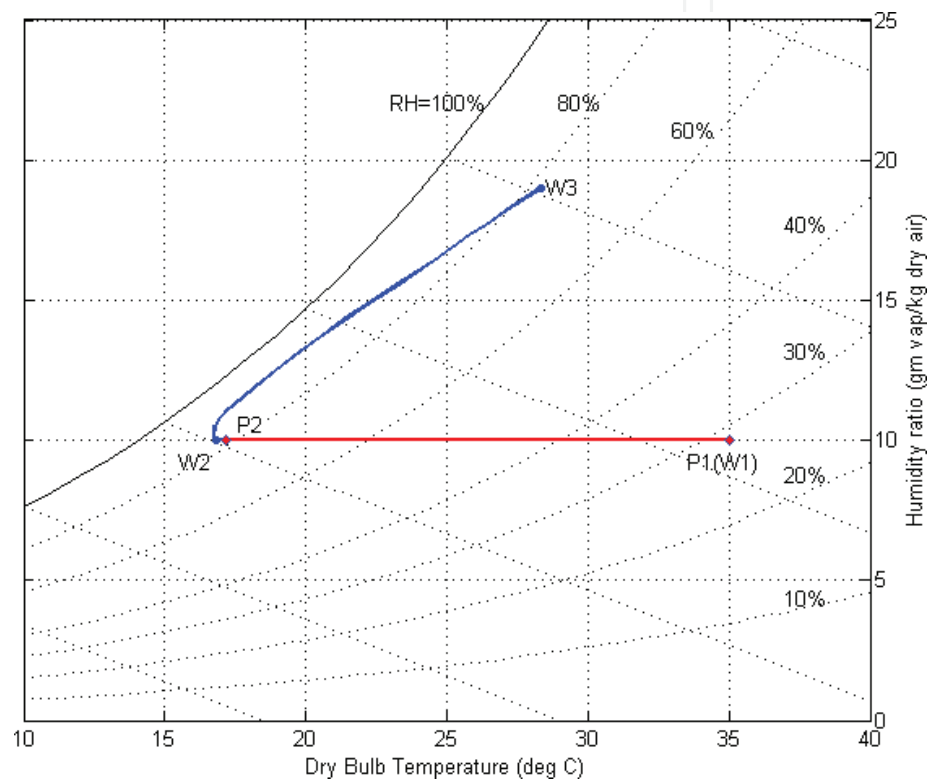


Figure 7. Illustration of air conditions on the psychrometric chart.

Parameters	Value	Units
$L$	1	m
$H_{product}$	6	mm
$H_{working}$	3	mm
$T_{air,in}$	35	°C
$\omega_{air,in}$	10	g/kg
$V_{product\ air}$	1	m/s
$V_{working\ air}$	1	m/s

Table 3. Pre-set conditions for the novel dew-point IEHX.

air (point P1 in **Figure 7**) are the same. In the product channel, the air dry-bulb temperature decreases with constant humidity ratio, resulting in a change of the condition from point P1 to point P2. In the working dry channel, sensible heat is transferred to the wet channel so that the working air temperature is reduced from state W1 to state W2. Since the air (at point W2 in **Figure 7**) is directed into the adjacent wet channel, it is humidified in the working wet channel where the heat is absorbed as a result of vaporizing water. The air in the working wet channel is finally exhausted at state W3.

**Figure 8** illustrates the dry-bulb temperature profiles in airflow passages including one product channel and two working channels. In both the working dry channel and the product channel, the air temperature decreases in the direction of the airflow. In the working wet channel, the lowest air temperature is achieved. It can be inferred from **Figure 8** that the heat is transferred from dry channels to working wet channels. The working air absorbs heat in the working wet channel resulting in a temperature increase along the flow direction in the wet channel [11].

5.3. Influence of inlet air temperature and humidity

**Figure 9** shows the wet-bulb effectiveness and dew-point effectiveness of the novel dew-point IEHX under different inlet air temperature and humidity conditions. In this study, the inlet air temperature varied in a range of values from 25 to 40°C and the humidity ratio was changed from 8 to 20 g/kg. The inlet air velocity and other geometry parameters were maintained as specified in **Table 3**.

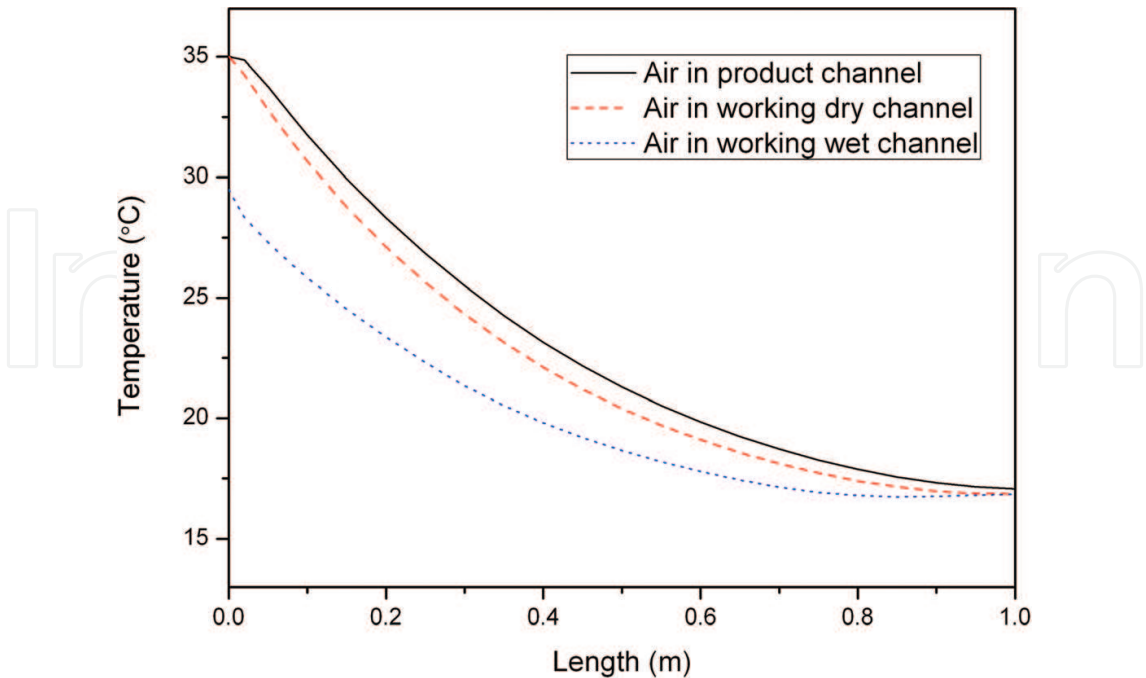


**Figure 8.** Temperature profiles of air in dry working channel, wet working channel, and product channel.

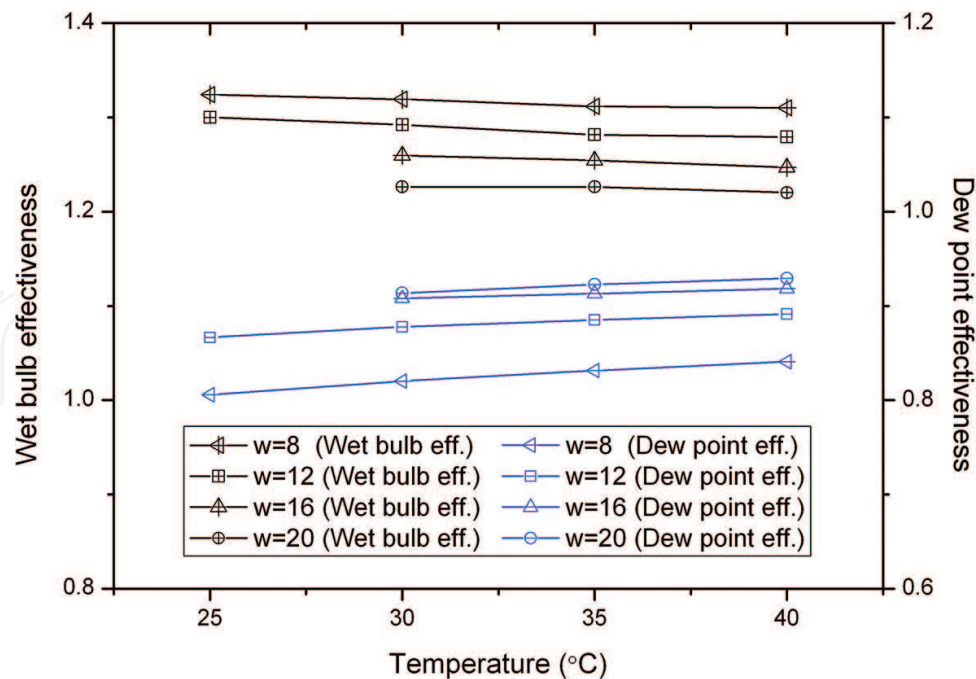


**Figure 9.** Cooling effectiveness for different inlet air conditions.

As shown in **Figure 9**, the dew-point effectiveness ranges 81–93%, and the wet-bulb effectiveness spans from 122 to 132%. Simulation results illustrate that the wet-bulb effectiveness of the IEHX is above 100%, which demonstrates the capability of the IEHX to produce air with a temperature lower than the wet-bulb temperature of inlet air.

When the inlet air humidity ratio is low, the vapor pressure gradient at the air-water interface is large resulting in a greater driving force for mass transfer. As a consequence, the working air is able to absorb more moisture during the process of vaporizing water, and the working air has a greater capacity to cool the air in adjacent dry channels. Therefore, a higher wet-bulb effectiveness can be reached by decreasing the inlet air humidity ratio.

Another finding from **Figure 9** is that the dew-point effectiveness may be decreased for a lower inlet air humidity ratio. It can be attributed to the following reason. As shown in the psychrometric chart, the dew-point temperature decreases significantly for a lower humidity ratio. Therefore, the temperature difference between the dew-point and the inlet dry bulb temperature shows a larger value at low humidity ratio [11].

#### 5.4. Influence of the channel dimension

The cooling efficiency of the IEHX is also affected by the channel height and channel length. Simulations have been conducted by using two types of the channel dimensions. For the first type, the height of product channel ( $H_{product}$ ) and the height of working channel ( $H_{working}$ ) were assumed as 6 and 3 mm, respectively, while maintaining the channel length ranging from 300 to 1500 mm. In the second type, the height of product channel ( $H_{product}$ ) and the height of

working channel ( $H_{working}$ ) were assumed as 10 and 5 mm, respectively, while maintaining the channel length spanning 300–2000 mm.

**Figure 10** illustrates the correlation between the dimensionless channel length ( $L/H_{working}$ ) and the wet-bulb effectiveness. It can be seen from the figure that the simulation results are consistent for the two sets of dimensions. A higher cooling efficiency can be achieved under a longer dimensionless channel length. In other words, increasing the channel length is able to improve the heat and mass transfer due to the increased contact area and time. Therefore, in order to achieve sub-wet-bulb cooling, the dimensionless channel length is suggested to be more than 200.

5.5. Thermal resistance analysis

**Table 4** indicates the thermal resistances with examples values for the counter-flow regenerative IEHX. The channel dimension significantly influences the thermal resistances due to convective heat transfer ( $R_1$  and  $R_4$ ). In addition, the modified thermal resistance for convective heat transfer in wet channel ( $R_4$ ) is impacted by the change of wet-bulb temperatures of the working air which also dominate the value of  $\xi$  ( $\xi = \frac{\Delta h}{\Delta T_{wb}}$ ). The Nusselt number can be acquired from the available literature [27] for fully developed laminar flow. For instance, the Nusselt number of 8.234 is employed for the fully developed laminar flow with parallel walls.

The impact of channel height on the thermal resistances for convective heat transfer ( $R_1$  and  $R_4$ ) is shown in **Figure 11**. The thermal resistance for conductive heat transfer in water film and plate is associated with the material and its thickness. **Figure 12** presents the impact of thickness on the thermal resistances for conductive heat transfer ( $R_2$  and  $R_3$ ). The IEHX can be made from a variety of materials [28, 29]. As shown in **Figures 11** and **12**, the thermal resistance

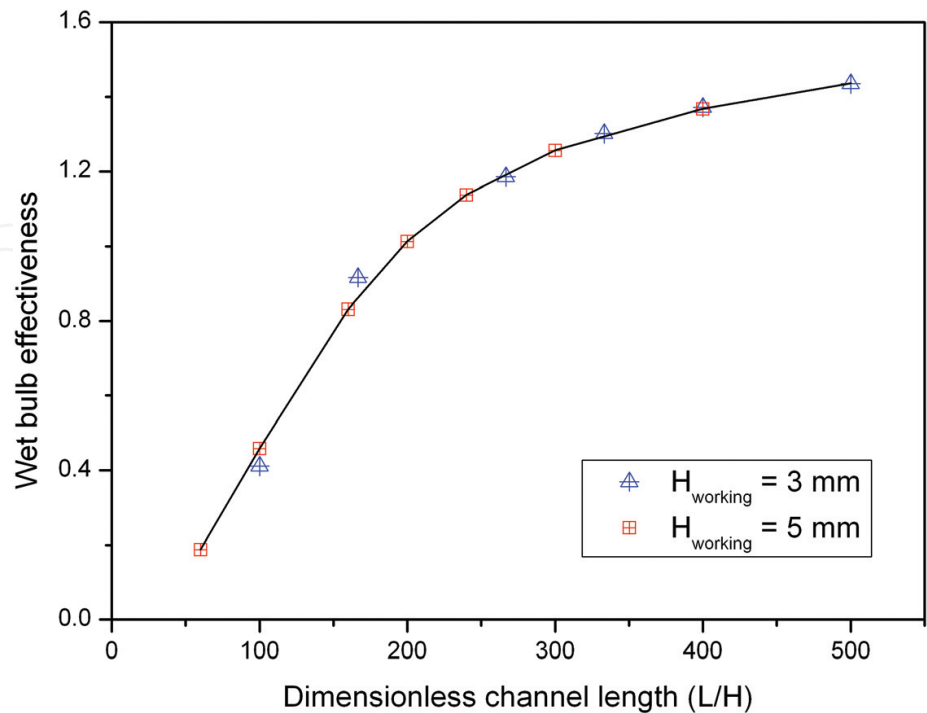


**Figure 10.** Impact of the dimensionless channel length on the cooling effectiveness.

Thermal resistance	Expression	Example values
$R_1$ : thermal resistance for dry channel	$R_1 = \frac{1}{h_c} = \frac{D_1}{Nu \cdot k}$	$R_1 = 0.045821 \text{ m}^2 \text{ K/W}$ , if $Nu = 8.235$ and $D_1 = 0.01 \text{ m}$
$R_2$ : thermal resistance for plate	$R_2 = \frac{\delta_p}{k_p}$	$R_2 = 1.48 \text{ E-}6 \text{ m}^2 \text{ K/W}$ , if $\delta_p = 3 \text{ mm}$ , and $k_p = 202 \text{ W/(m K)}$
$R_3$ : thermal resistance for water film	$R_3 = \frac{\delta_w}{k_w}$	$R_3 = 4.92 \text{ E-}4 \text{ m}^2 \text{ K/W}$ , if $\delta_w = 3 \text{ mm}$
$R_4$ : modified thermal resistance for wet channel	$R_4 = \frac{1}{\xi h_m} = \frac{c_{pa} D_2}{\xi Nu k}$	$R_4 = 0.013612 \text{ m}^2 \text{ K/W}$ , if $Nu = 8.235$ , $D_2 = 0.01 \text{ m}$ , and $\xi = 3.4 \text{ kJ/(kg K)}$

Table 4. Thermal resistances in the IEHX.

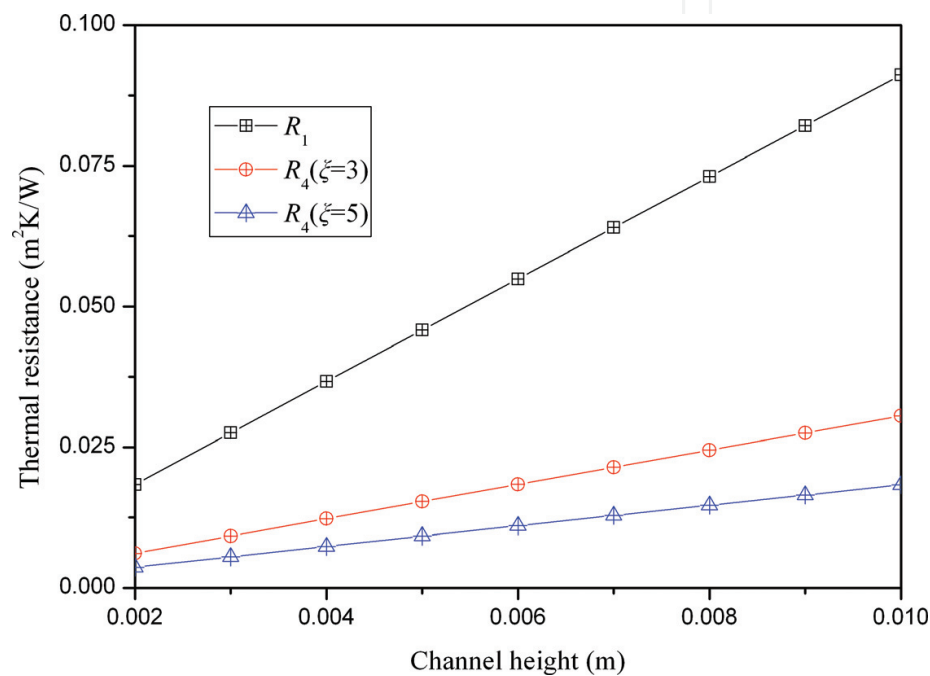


Figure 11. Thermal resistance for convective heat transfer under varying channel height.

$R_2$  is relatively small compared with the thermal resistance  $R_1$  and  $R_4$ , especially when the plate has a small thickness. In general, the thermal resistances for convection heat transfer are much larger than the thermal resistances for conduction. Therefore, the thermal resistance  $R_2$  and  $R_3$  have marginal influence on the overall heat transfer of the whole system [7].

According to the analysis on thermal resistances, following suggestions are obtained in order to enhance the cooling performance of the IEHX. The airflow channels may be redesigned to generate larger flow turbulence resulting in a lower thermal resistance so that a larger heat transfer coefficient can be achieved [30]. The Reynolds number of the airflow in this IEHX is close to 1100. Therefore, the channel can be modified to create the flow turbulence by installing physical ribs in the airflow channels, which could potentially reduce the thermal resistance and increase the Reynolds number above 3000. In addition, the IEHX with a smaller hydraulic diameter will positively influence its cooling effectiveness due to a higher Nusselt number. To enhance the mass transfer process due to water evaporation in wet channels, some techniques may be employed involving increasing the water vapor concentration gradient between the water surface and the air stream.



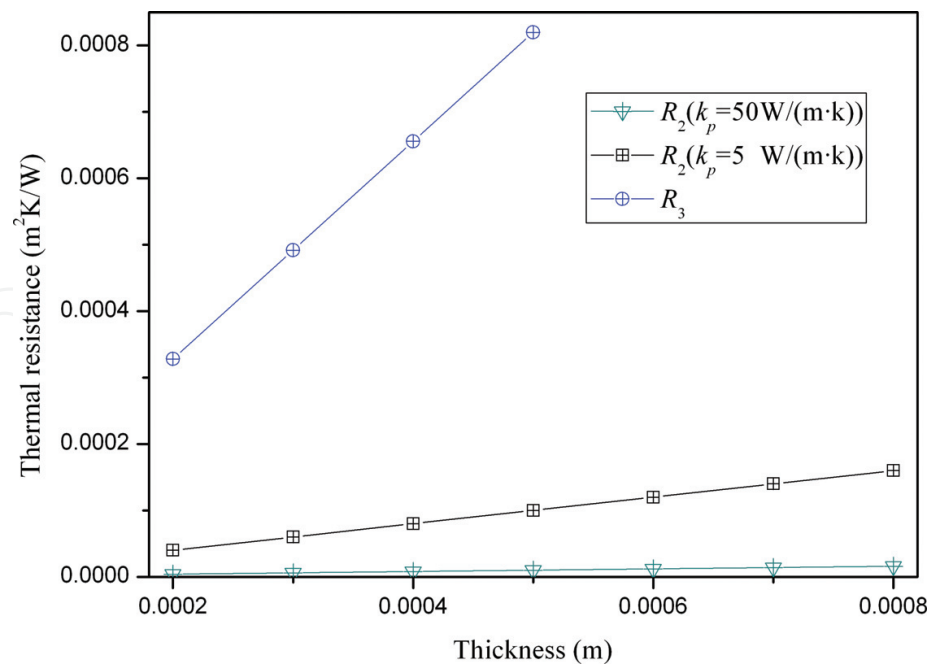


Figure 12. Thermal resistance for conduction in plate and water film.

6. Conclusions

The performance of novel indirect evaporative heat exchangers has been investigated. We developed a numerical model to study the influences of several parameters on the cooling performance. Wet-bulb and dew-point effectiveness were employed to evaluate the cooling efficiency of the IEHX. The cooling performance was impacted by the operating conditions and the structure of airflow passages. To promote cooling effectiveness, suggestions are provided to improve the thermal performance of the cooler. To achieve a lower thermal resistance, it is possible to modify the IEHX's channel and to create larger airflow turbulence. In addition, the performance of the IEHX can be positively improved by employing a geometry with a smaller hydraulic diameter.

Author details

Xin Cui, Xiaohu Yang, Yanjun Sun, Xiangzhao Meng and Liwen Jin\*

\*Address all correspondence to: lwjin@xjtu.edu.cn

Institute of Building Environment and Sustainable Technology, Shaanxi Engineering Research Center of Building Environment and Energy, School of Human Settlements and Civil Engineering, Xi'an Jiaotong University, Xi'an, Shaanxi, China

## References

- [1] Duan Z, Zhan C, Zhang X, Mustafa M, Zhao X, Alimohammadisagvand B, et al. Indirect evaporative cooling: Past, present and future potentials. *Renewable and Sustainable Energy Reviews*. 2012;**16**:6823-6850. DOI: 10.1016/j.rser.2012.07.007
- [2] Chua KJ, Chou SK, Yang WM, Yan J. Achieving better energy-efficient air conditioning—A review of technologies and strategies. *Applied Energy*. 2013;**104**:87-104. DOI: 10.1016/j.apenergy.2012.10.037
- [3] Jaber S, Ajib S. Evaporative cooling as an efficient system in Mediterranean region. *Applied Thermal Engineering*. 2011;**31**:2590-2596. DOI: 10.1016/j.applthermaleng.2011.04.026
- [4] Caliskan H, Dincer I, Hepbasli A. A comparative study on energetic, exergetic and environmental performance assessments of novel M-cycle based air coolers for buildings. *Energy Conversion and Management*. 2012;**56**:69-79. DOI: 10.1016/j.enconman.2011.11.007
- [5] Cui X, Chua KJ, Yang WM. Numerical simulation of a novel energy-efficient dew-point evaporative air cooler. *Applied Energy*. 2014;**136**:979-988. DOI: 10.1016/j.apenergy.2014.04.040
- [6] Maisotsenko V, Gillan LE, Heaton TL, Gillan AD. Method and plate apparatus for dew point evaporative cooler. US Patent 6,508,402. 2003
- [7] Cui X, Chua KJ, Islam MR, Yang WM. Fundamental formulation of a modified LMTD method to study indirect evaporative heat exchangers. *Energy Conversion and Management*. 2014;**88**:372-381. DOI: 10.1016/j.enconman.2014.08.056
- [8] Cui X, Islam MR, Mohan B, Chua KJ. Developing a performance correlation for counter-flow regenerative indirect evaporative heat exchangers with experimental validation. *Applied Thermal Engineering*. 2016;**108**:774-784. DOI: 10.1016/j.applthermaleng.2016.07.189
- [9] Cui X, Chua KJ, Islam MR, Ng KC. Performance evaluation of an indirect pre-cooling evaporative heat exchanger operating in hot and humid climate. *Energy Conversion and Management*. 2015;**102**:140-150. DOI: 10.1016/j.enconman.2015.02.025
- [10] Hasan A. Going below the wet-bulb temperature by indirect evaporative cooling: Analysis using a modified  $\varepsilon$ -NTU method. *Applied Energy*. 2012;**89**:237-245. DOI: 10.1016/j.apenergy.2011.07.005
- [11] Cui X, Chua KJ, Yang WM, Ng KC, Thu K, Nguyen VT. Studying the performance of an improved dew-point evaporative design for cooling application. *Applied Thermal Engineering*. 2014;**63**:624-633. DOI: 10.1016/j.applthermaleng.2013.11.070
- [12] Liu Z, Allen W, Modera M. Simplified thermal modeling of indirect evaporative heat exchangers. *HVAC&R Research*. 2013;**19**:257-267. DOI: 10.1080/10789669.2013.763653

- [13] Lee J, Choi B, D-YY L. Comparison of configurations for a compact regenerative evaporative cooler. *International Journal of Heat and Mass Transfer*. 2013;**65**:192-198. DOI: 10.1016/j.ijheatmasstransfer.2013.05.068
- [14] Cui X, Islam MR, Mohan B, Chua KJ. Theoretical analysis of a liquid desiccant based indirect evaporative cooling system. *Energy*. 2016;**95**:303-312. DOI: 10.1016/j.energy.2015.12.032
- [15] Cui X, Chua KJ, Yang WM. Use of indirect evaporative cooling as pre-cooling unit in humid tropical climate: An energy saving technique. *Energy Procedia*. 2014;**61**:176-179. DOI: 10.1016/j.egypro.2014.11.933
- [16] Anisimov S, Pandelidis D. Theoretical study of the basic cycles for indirect evaporative air cooling. *International Journal of Heat and Mass Transfer*. 2015;**84**:974-989. DOI: 10.1016/j.ijheatmasstransfer.2015.01.087
- [17] Zhao X, Li JM, Riffat SB. Numerical study of a novel counter-flow heat and mass exchanger for dew point evaporative cooling. *Applied Thermal Engineering*. 2008;**28**:1942-1951. DOI: 10.1016/j.applthermaleng.2007.12.006
- [18] Moshari S, Heidarinejad G. Numerical study of regenerative evaporative coolers for sub-wet bulb cooling with cross- and counter-flow configuration. *Applied Thermal Engineering*. 2015;**89**:669-683. DOI: 10.1016/j.applthermaleng.2015.06.046
- [19] Jradi M, Riffat S. Experimental and numerical investigation of a dew-point cooling system for thermal comfort in buildings. *Applied Energy*. 2014;**132**:524-535. DOI: 10.1016/j.apenergy.2014.07.040
- [20] Ham S-W, Jeong J-W. DPHX (dew point evaporative heat exchanger): System design and performance analysis. *Energy*. 2016;**101**:132-145. DOI: 10.1016/j.energy.2016.02.019
- [21] Moshari S, Heidarinejad G, Fathipour A. Numerical investigation of wet-bulb effectiveness and water consumption in one-and two-stage indirect evaporative coolers. *Energy Conversion and Management*. 2016;**108**:309-321. DOI: 10.1016/j.enconman.2015.11.022
- [22] Chen Y, Yang H, Luo Y. Indirect evaporative cooler considering condensation from primary air: Model development and parameter analysis. *Building and Environment*. 2016;**95**:330-345. DOI: 10.1016/j.buildenv.2015.09.030
- [23] Woods J, Kozubal E. A desiccant-enhanced evaporative air conditioner: Numerical model and experiments. *Energy Conversion and Management*. 2013;**65**:208-220. DOI: 10.1016/j.enconman.2012.08.007
- [24] Riangvilaikul B, Kumar S. An experimental study of a novel dew point evaporative cooling system. *Energy and Buildings*. 2010;**42**:637-644. DOI: 10.1016/j.enbuild.2009.10.034
- [25] ASHRAE. *ASHRAE Handbook-Fundamentals*. Atlanta, GA: American Society of Heating, Refrigerating and Air-Conditioning Engineers; 2009
- [26] Kozubal E, Woods J, Judkoff R. Development and analysis of desiccant enhanced evaporative air conditioner prototype (No. NREL/TP-5500-54755). National Renewable Energy Laboratory (NREL); 2012

- [27] Kays WM, Crawford ME, Weigand B. Convective Heat and Mass Transfer. 4th ed. New York: McGraw-Hill Higher Education; 2005
- [28] Al-Sulaiman F. Evaluation of the performance of local fibers in evaporative cooling. Energy Conversion and Management. 2002;**43**:2267-2273. DOI: 10.1016/S0196-8904(01)00121-2
- [29] Zhao X, Liu S, Riffat SB. Comparative study of heat and mass exchanging materials for indirect evaporative cooling systems. Building and Environment. 2008;**43**:1902-1911. DOI: 10.1016/j.buildenv.2007.11.009
- [30] Alam T, Saini RP, Saini JS. Use of turbulators for heat transfer augmentation in an air duct — A review. Renewable Energy. 2014;**62**:689-715. DOI: 10.1016/j.renene.2013.08.024

IntechOpen

